

On the effects of strong ionization in medium-order harmonic generation

M. BELLINI,^{1,2} C. CORSI,² AND M.C. GAMBINO³

¹Istituto Nazionale di Ottica Applicata, Largo E. Fermi, 6, I-50125 Florence, Italy

²European Laboratory for Non Linear Spectroscopy (LENS) and INFN, Largo E. Fermi, 2, I-50125 Florence, Italy

³Department of Physics, University of Florence, Largo E. Fermi, 2, I-50125 Florence, Italy

(RECEIVED 6 November 2001; ACCEPTED 9 December 2001)

Abstract

Strong ionization of the gas medium has significant effects in the process of medium-order harmonic generation. The combined effect of neutral atom depletion and defocusing of the pump beam due to the intensity-dependent density of free electrons, significantly modifies the conversion characteristics and efficiency. For moderate harmonic orders, the yield is optimized for well-defined values of the pump laser intensity that do not depend on the order or on the focusing geometry, but only on the ionization potential of the gas. In particular focusing conditions, the ionization-induced defocusing can effectively guide the pump beam along channels of optimum intensity, thus enhancing the overall conversion efficiency. We demonstrate that a very simple model is able to reproduce all our experimental results in a surprisingly good way.

Keywords: Beam propagation; High-order harmonic generation; Strong-field ionization; Ultrashort laser pulses

1. INTRODUCTION

High-order harmonics have now become a well-established source of pulsed coherent radiation in the short-wavelength region of the electromagnetic spectrum (for a recent review, see Salières *et al.*, 1999). By the interaction of a short and intense visible laser pulse with the atoms of a supersonic jet, odd-order harmonics of the fundamental laser frequency are generated and, depending on the pulse characteristics and on the ionization potential of the atoms, very high orders can be efficiently generated at wavelengths down to the XUV or to the soft X-ray regions.

The now commonly available 100-fs, high-repetition rate, millijoule-level, Ti:Sa amplified laser systems are a particularly well-suited source for the generation of medium-order harmonics. Such relatively low orders are the most interesting for the extension of high-resolution spectroscopic studies of atoms, molecules, and ions to the short-wavelength regime (Bellini *et al.*, 2001). To increase the laser peak intensity available in the focus (to improve the harmonic yield) and to decrease it on the monochromator-grating (not to damage it), relatively high numerical aper-

tures are normally used in these situations, with confocal parameters of the laser beam comparable to the length of the gas jet. Heavy (and easy to ionize) noble gases are often chosen as the generating medium in this wavelength range thanks to their higher conversion efficiency. In such cases, a strong medium ionization is always present and, though ionized electrons are indeed necessary for harmonic generation to take place, their massive presence can pose serious limits to the possibility of extending the generation process toward higher yields and shorter wavelengths by increasing the interaction intensity.

In this article, we study in a detailed way the effects of strongly ionized, heavy noble gases (argon and xenon) on the generation efficiency of medium-order harmonics. We show that only “geometrical” effects of medium ionization seem to play a significant role in these situations, determining the conditions for best harmonic conversion. An extremely simple model is introduced that seems to fully explain the observed behavior.

2. EXPERIMENT

The experimental setup (Bellini *et al.*, 2001*b*) is sketched in Figure 1 and is composed of a vacuum chamber equipped with an electromagnetic valve for the interaction between

Address correspondence and reprint requests to: M. Bellini, Istituto Nazionale di Ottica Applicata, Largo E. Fermi, 6, I-50125 Florence, Italy.
E-mail: bellini@ino.it

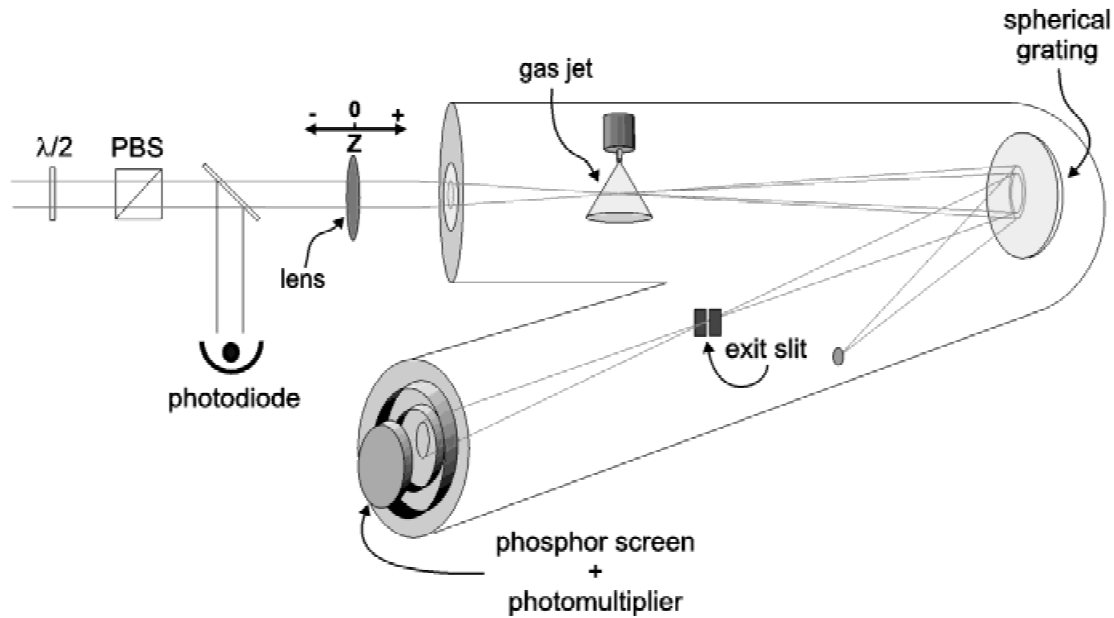


Fig. 1. Experimental setup.

the laser pulses and the gas jet, and a vacuum monochromator for the spectral selection of the different harmonic orders produced. The Ti:Sa amplified laser system provides 0.7-mJ, 100-fs pulses centered around 800 nm and with a 1-kHz repetition rate. Xenon and argon have been used for the experiments at a constant backing pressure of about 1.5 bar. Harmonics have been observed downstream of the exit slit of the monochromator by means of a phosphor screen and a photomultiplier. A photodiode, receiving a small fraction of the pump laser light, has been used to monitor the laser pulse energy.

Two lenses, of 150 and 200 mm focal lengths, have been used to focus the laser pulses inside the interaction chamber. The distance between the laser focus and the gas jet has been varied by moving the lenses along the propagation direction, defined as z , by means of a translation stage. By defining the position $z = 0$ as the location of the gas jet, positive values of z mean that the laser is focused beyond the jet and that the beam interacts with the atoms while converging towards the waist. On the other hand, negative values of z mean that the waist is before the jet and that the beam is diverging when it encounters the atoms.

3. DEPLETION EFFECTS

When the intensity of the laser reaches the so-called saturation intensity I_s , a significant fraction of the neutral atoms in the medium has been depleted and the generation process essentially stops. The neutral atom density $N(t)$ can be found to decrease in a laser pulse with time profile $I(t)$ as

$$N(t) = N_0 e^{-\int_{-\infty}^t W(I(t')) dt'}, \quad (1)$$

where $W(I(t))$ is the ionization rate of the atoms. The saturation intensity I_s can then be defined for a given gas as the minimum laser peak intensity for which the neutrals have been completely depleted at the end of the pulse. The saturation intensities for an 800-nm, 100-fs FWHM, Gaussian pulse in xenon and argon result, respectively, $I_s(\text{Xe}) = 1.5 \times 10^{14} \text{ W/cm}^2$, and $I_s(\text{Ar}) = 3.5 \times 10^{14} \text{ W/cm}^2$. Figure 2 shows the neutral density profile in xenon for different values of the peak intensity of a 100-fs laser pulse.

A saturation in the conversion efficiency can be observed experimentally in Figure 3, where a logarithmic plot of the harmonic yield as a function of the laser intensity is shown for the 13th harmonic in Xe. The curve has a clear exponential behavior with two different growing rates separated by a net knee where the curve drastically changes slope. Very similar behaviors have been observed for several harmonics in the plateau with both xenon and argon. The intensities at which the curves change slope are always in good agreement with those found above for the saturation intensities of the two gases.

If we assume that harmonic emission is only limited by the medium length and that the gas pressure in the jet is constant, then the final number of harmonic photons scales linearly with the transverse section $S(z)$ (recall that z is the relative distance between the gas jet and the laser focus) and quadratically with the length L of interaction with the gas jet. It can thus be modeled as

$$N_h(z, P) \propto f(I(z, P)) S(z) L^2, \quad (2)$$

where $I(z, P)$ is the pulse peak intensity at position z and for an average laser power P , and the function $f(I(z, P))$ is defined as

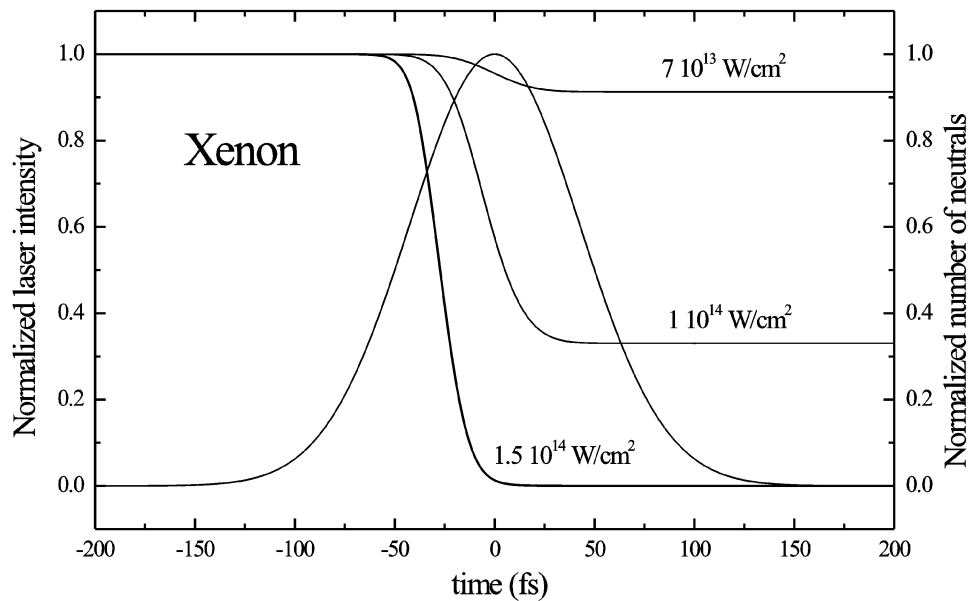


Fig. 2. Normalized neutral atom density for various values of the laser peak intensity of a 100-fs pulse in xenon. Also shown is the normalized intensity profile of the pulse.

$$f(I(z, P)) = \begin{cases} I(z, P)^p & \text{if } I(z, P) < I_s \\ \frac{I_s^p}{I_s^s} I(z, P)^s & \text{if } I(z, P) \geq I_s, \end{cases} \quad (3)$$

in order to model the experimental behavior found above (see Fig. 3). The parameter p is the exponent in the non-saturated regime, while s is the exponent for the situation where saturation is present.

If the average laser power P is kept constant, the first two factors in Eq. (2) depend on the beam waist size at position z : for large values of $|z|$ (i.e., far from the focus) the waist is large and the laser intensity is lower than the saturation intensity. In these conditions, it is convenient to decrease $|z|$, as the effect of a smaller interaction volume is overcompensated by the rapid exponential growth of the harmonic yield with increasing laser intensity. However, when $|z|$ is

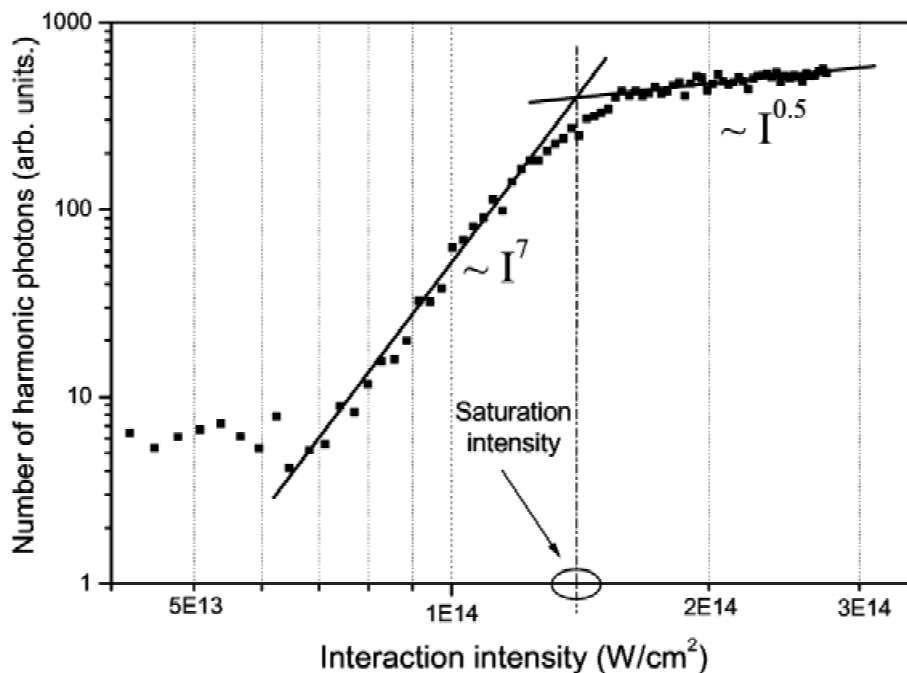


Fig. 3. Yield of the 13th harmonic in xenon as a function of the pump laser intensity. Two regions with very different slopes are evident.

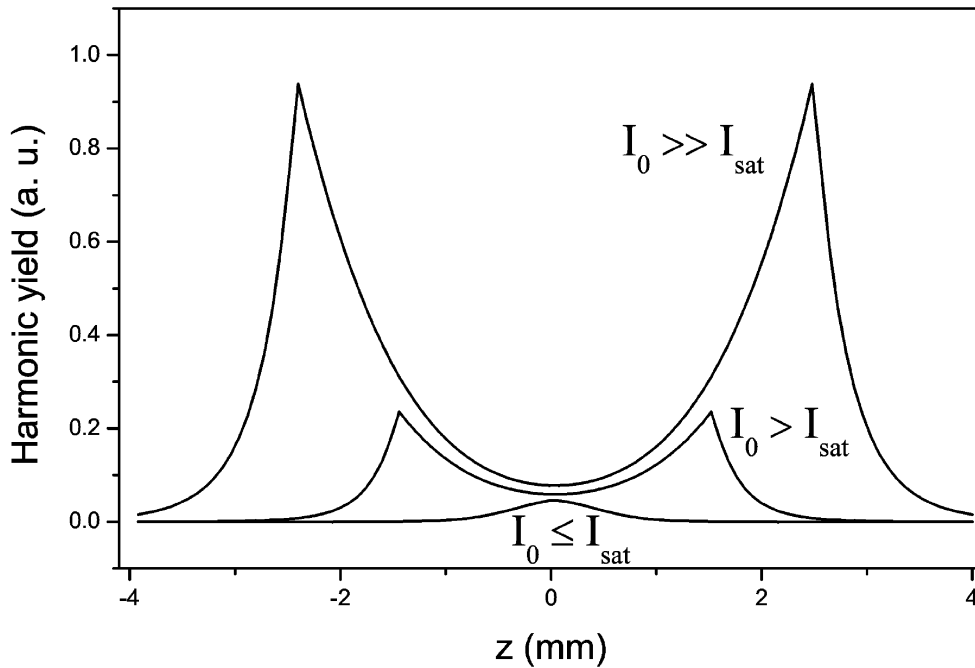


Fig. 4. Calculated harmonic yields as a function of the position z for various values of the laser peak intensity, above and below I_s .

so small that the laser intensity reaches saturation, the harmonic yield almost stops growing with the pump intensity and the main contribution now comes from the decreasing interacting volume: Going toward the focus only has the result of diminishing the number of atoms available for harmonic generation.

The overall dependence of $N_h(z, P)$ on z at a constant value of P shows a symmetric double peak centered around $z = \pm z_s(P)$, where $z_s(P)$ is the position along the propagation axis where the pulse reaches the saturation intensity (see Fig. 4). Using a Gaussian beam with a peak intensity of I_0 and a waist w_0 in the focus, these points are easily found as

$$z_s(P) = \frac{\pi w_0^2}{\lambda} \sqrt{\frac{I_0(P)}{I_s} - 1}. \tag{4}$$

Of course, when the pulse energy is so low that, even at the focus, I_0 is lower than the saturation intensity, then the above equation has no real solution and the curve shows a single central peak at $z = 0$. So, as expected, for low pulse energies, the best conversion efficiency is obtained by placing the laser focus directly below the gas jet.

The same qualitative behavior can be found for a wide range of exponents p and s : The locations of maxima keep following the contour lines corresponding to $I(z, P) = I_s$ as long as $p > 2$ and $s < 2$.

Figure 5 presents an experimental 3D plot which is representative of the general behavior of the overall harmonic yield as a function of the relative focus–jet position and of the laser average power: a single peak at $z = 0$ for low pump power, and a bifurcation into two peaks (almost symmetric

around $z = 0$ but with quite different heights) for higher incoming powers. The positions of the most intense right peak, located at $z > 0$ (when the laser focuses beyond the gas jet), are also reported in Figure 6 superposed to the experimental contour plots of the peak laser intensity for various combinations of harmonic orders, focusing lenses, and atomic

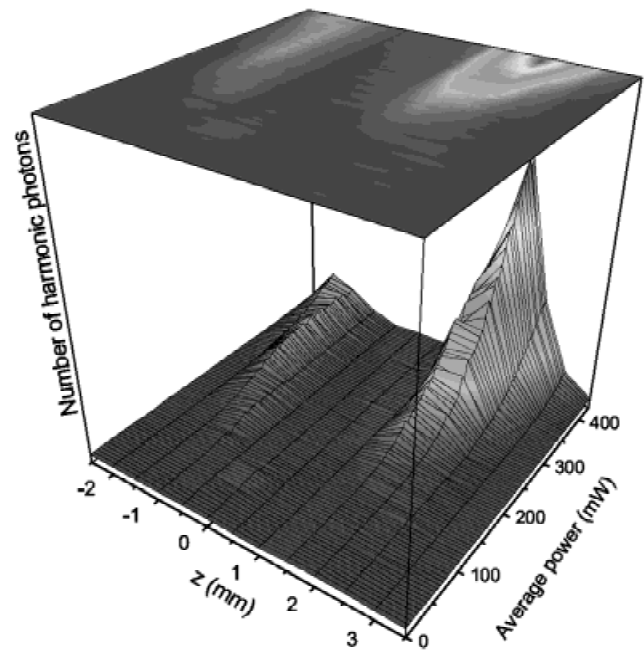


Fig. 5. Three dimensional plot of the measured 13th harmonic yield as a function of the average laser power and of the relative focus–jet distance.

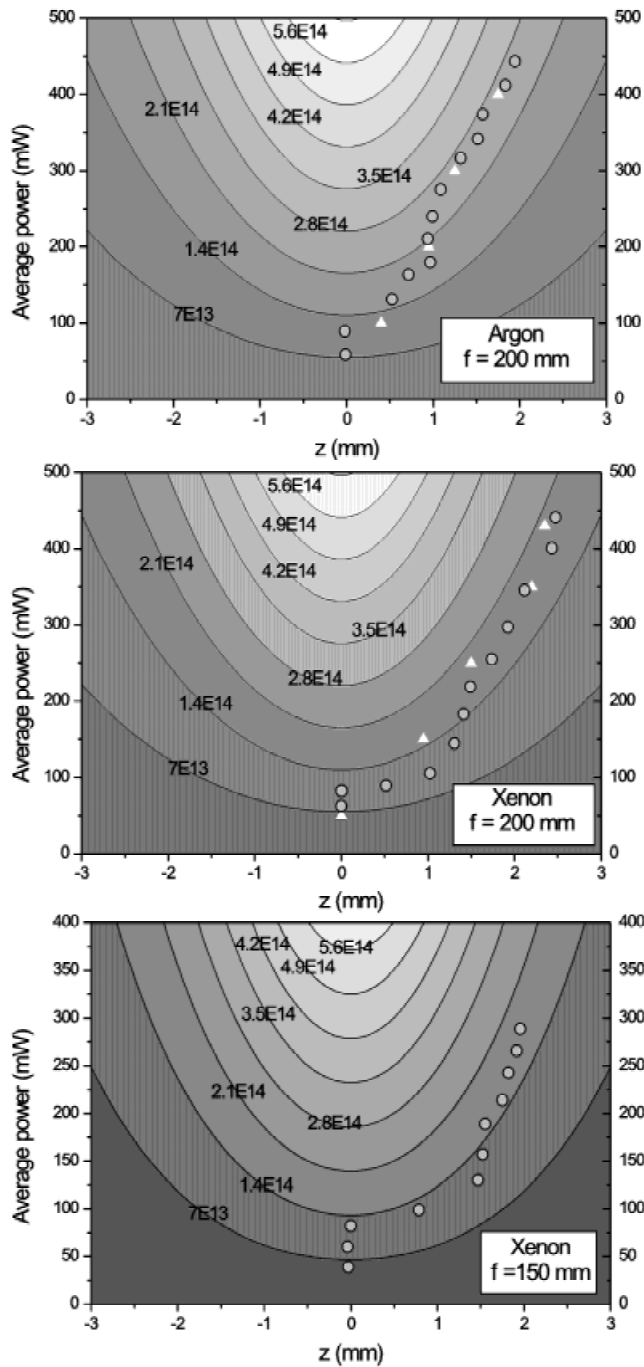


Fig. 6. Positions of the measured peaks in the harmonic conversion efficiency. In the three figures the circular and triangular data points are relative to the 13th and to the 5th harmonics, respectively.

media. In all cases, the peaks are located at $z = 0$ for low powers, and then, after some initial deviations, follow almost exactly contour lines of constant intensity when the power is increased. These intensities do not show a significant dependence on the harmonic order, but they clearly depend on the gas used for the generation and are the same with different focusing lenses. The limit intensities found for argon and xenon are 2.8×10^{14} and 1.6×10^{14} W/cm²,

respectively. The previous explanation based on the depletion effects due to ionization accounts for the observed behavior.

Structures with multiple maxima of the harmonic conversion efficiency as a function of z have been predicted and observed by several authors in a range of different experimental conditions and have been often interpreted as effects related to the phase-matching between the pump and the harmonic field (see, e.g., L’Huillier & Balcou, 1993; Balcou & L’Huillier, 1993; Lewenstein *et al.*, 1995; Bouhal *et al.*, 1998). Such factors, closely related to the phase shift induced by focusing, to the atomic dipole phase, and to the phase mismatch induced by plasma dispersion, are strongly dependent on the harmonic order and start to limit the conversion efficiency only for sufficiently high harmonics.

The fact that in our experimental conditions only the ionization potential of the gas determines the optimum intensity for harmonic generation, independently from the order, seems to imply that phase-matching does not limit harmonic conversion in this case.

4. DEFOCUSING EFFECTS

The strong asymmetry in the heights of the left and right peaks shown in Figure 5 is probably connected to the defocusing induced by free electrons on the fundamental laser field. Due to the strong spatial dependence of the intensity profile of the pulses, a spatial phase modulation is imparted on the laser. This, in turn, results in self-defocusing of the beam that can substantially modify the propagation through the ionized sample (Rankin *et al.*, 1991; Monot *et al.*, 1992) and affect the conversion efficiency by limiting the laser intensity achievable in the ionizing medium to a value much lower than I_0 .

The effect of laser beam defocusing on harmonic generation has already been pointed out by Rae (1993), Rae *et al.* (1994), and Altucci *et al.* (1996), and it has been analyzed in some more detail by Sakai and Miyazaki (1994) and Miyazaki and Takada (1995). Here we concentrate on the same geometrical effects of ionization, but we give some general relationships that may allow us to relate all the observed structures to the experimental parameters in a simple way.

We can start by expressing the phase shift suffered on axis by the laser beam after it passes through a length L of ionized medium as

$$\Delta\phi_e = -\frac{\pi L}{\lambda} \frac{N_e}{N_c}, \tag{5}$$

where N_e is the electron density and N_c is the critical density given by

$$N_c = \frac{m\epsilon_0\omega^2}{e^2}. \tag{6}$$

This means that the phase of the central ray of the beam is advancing with respect to the phase of off-axis points (where we may consider the electron density negligible). The beam acquires a positive wavefront curvature and will tend to diverge. This phase shift (or wavefront curvature) has to be compared to that intrinsic to a focused Gaussian beam $\Delta\phi_G = z/z_R$ (where $z_R = \pi\omega_0^2/\lambda$ is the Rayleigh range of the beam) and the two contributions have to be summed together to give the overall behavior of the beam. The total on-axis phase for each (z, P) point in the relative focus–jet position and pulse-peak-power space is then given by

$$\Delta\phi(z, P) = \frac{z}{z_R} - \frac{\pi L}{\lambda} \frac{N_e(z, P)}{N_c}. \quad (7)$$

With these simple assumptions, we can immediately explain the asymmetry between the left and right peaks in Figure 5. When $z > 0$, the two terms in Eq. (7) have opposite signs and tend to compensate each other, while for $z < 0$ they add their contributions to a large negative on-axis phase. In other words, when we place the ionized medium in the converging part of the focused beam, it acts as a divergent lens that tends to collimate it and to maintain the interaction intensity at the optimum value throughout the gas sample. If, on the other hand, the gas jet is placed downstream of the focus, it further increases the divergence of the beam, causing a drop in the intensity and effectively limiting the length of interaction with the gas (see Fig. 7).

We can assume that placing the ionized medium at a position z along the propagation direction of the unperturbed Gaussian beam transforms it into another Gaussian beam with different parameters (Bellini *et al.*, 2001a). In particular we can find the new beam divergence at the exit of the ionized gas medium as

$$\theta_{new}(z, P) = -\frac{\lambda\Delta\phi(z, P)}{\pi w(z)}. \quad (8)$$

And we can define the effective interaction length with the medium as that over which the relative intensity variations are less than η :

$$L_{eff}(z, P) = \frac{\eta w(z)}{2|\theta_{new}(z, P)|}. \quad (9)$$

Of course $L_{eff}(z, P)$ cannot exceed the length of the medium itself and must be upper-limited to L . We can now combine Eqs. (9) and (2) to find the total harmonic yield as a function of z and P in the presence of ionization-induced defocusing:

$$N_h(z, P) \propto f(I(z, P))S(z)L^2\left(\frac{L_{eff}(z, P)}{L_{eff}(z, 0)}\right)^2. \quad (10)$$

The last term is a scaling factor that we introduce to keep the defocusing effects into account.

In Figure 8, we show the measured and calculated 13th harmonic yield in argon as a function of z at fixed laser input power. The two calculated peaks can now well reproduce the experimental asymmetry, and the positions, shapes, and relative intensities of the two maxima are fairly well matched.

The effect of the strong defocusing of the beam due to the presence of free electrons is also evident in other peculiar behaviors, such as the strongly nonmonotonous dependence of the harmonic yield on the pump laser intensity in $z = 0$, or the deviations of the points of maximum efficiency from the laser isointensity lines at low pulse energy (see Fig. 9).

It should be emphasized that the calculated curves in Figures 8 and 9 are not best fits to the data, but have been directly obtained from Eq. (10) using only the experimentally available parameters. The only remaining arbitrariness is in the parameter η used in the definition of the effective interaction length, but we have found that a single value of $\eta \approx 20\%$ is able to reproduce well all the measured data, regardless of the different experimental situations.

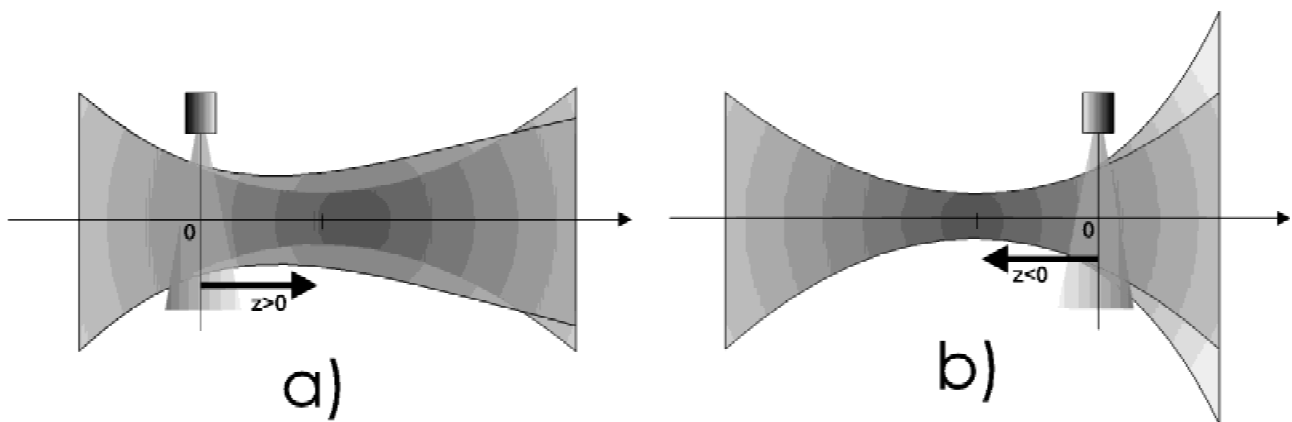


Fig. 7. Illustration of the effects of strong ionization-induced defocusing in the two situations of a) “jet before the focus” and b) “jet after the focus”. In the first case the laser is re-collimated and keeps the optimal interaction intensity for longer distances, while in the second case the beam divergence is further increased and strongly limits the interaction length.

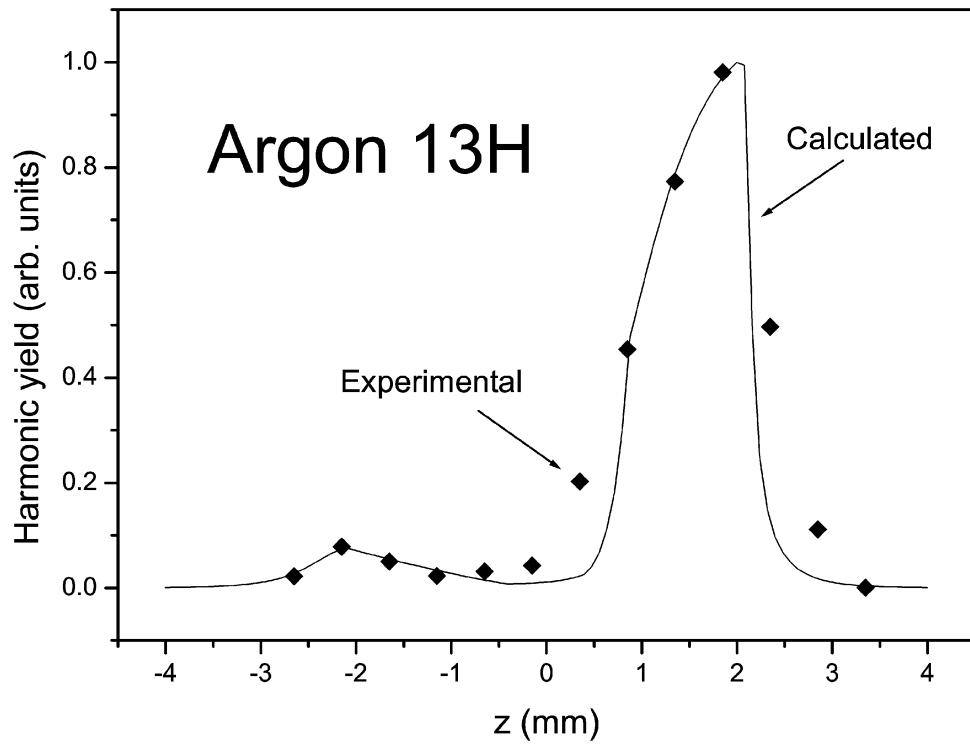


Fig. 8. Experimental and calculated profiles of harmonic yield in argon as a function of the focus-jet relative position at a fixed laser pulse energy. The defocusing induced by free electrons improves the conversion efficiency when the gas jet is located before the laser focus ($z > 0$) and strongly suppresses it for $z < 0$.

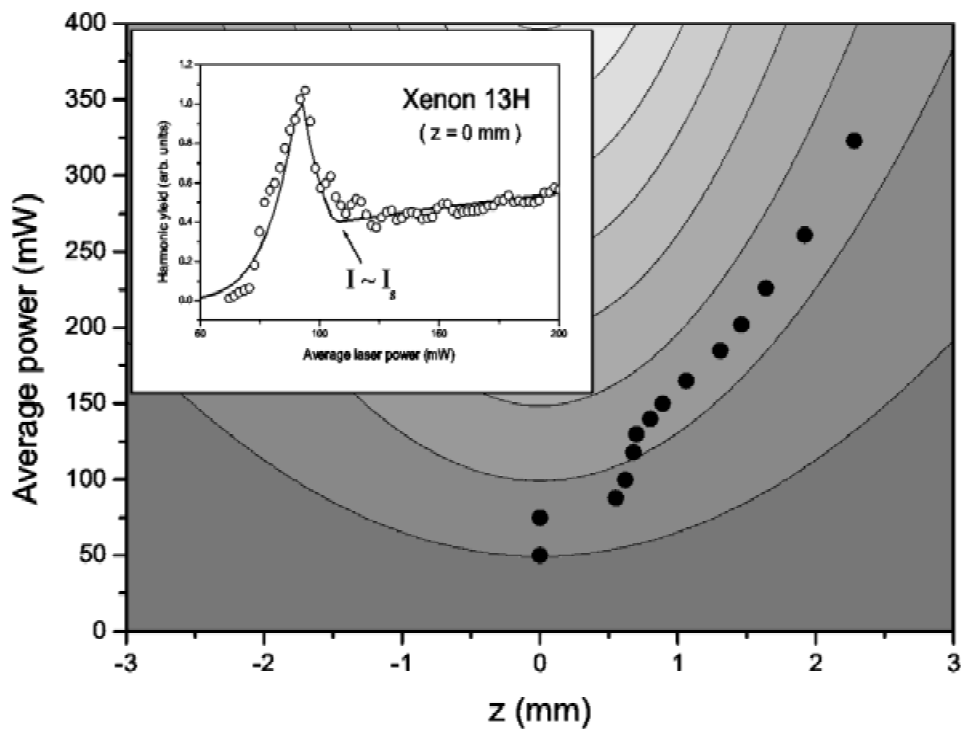


Fig. 9. Calculated positions of the harmonic-yield peaks for xenon and for a 200-mm focusing lens: the situation is the same of the middle plot of Fig. 6. The inset shows the measured and calculated yield of the 13th harmonic in xenon when the laser focus is placed directly below the gas nozzle.

Of course, the agreement between measured and calculated data is not perfect, but, keeping in mind the crude assumptions used and the intrinsic discontinuities present in our model, it is surprising to find that it is possible to reproduce the experimental results so well.

5. CONCLUSIONS

In conclusion, we have shown that the process of medium-order harmonic generation in strongly ionized media can be well understood and its properties can be accurately predicted on the basis of a simple model. For the intensities and the harmonic orders considered here, the only important contribution to the harmonic yield arises from the combined effect of neutral medium depletion and defocusing of the pump laser beam.

By changing both the laser pulse energy and the relative position between the gas jet and the laser focus, we find that the positions of maximum efficiency follow contour lines of constant intensity and that this is closely related to the saturation intensity of the gas. By noting that the observed features do not depend on the harmonic order but only on the ionization potential of the gas, we also find that, in these experimental conditions, the main contribution to the conversion efficiency dependence on the focus-jet position is not given by phase-matching effects but by the depletion of the neutral medium.

The observed asymmetries in the efficiency plots are explained as the result of defocusing of the pump beam due to the presence of free electrons. While in most cases this can reduce the overall efficiency, we find that in some conditions it can actually enhance it by forming channels of almost constant optimum intensity. Also in this case, we are able to reproduce in a good qualitative way all the experimental results by means of our simple model. Other peculiar features, such as the strongly nonmonotonous dependence of the harmonic yield on the pump laser intensity under particular experimental conditions, can be clearly explained and are well reproduced by our simulations.

We believe that these experimental results and the simple model introduced to explain them will be of use for the efficient production of medium-order harmonics with the systems now widely available in laboratories around the world. Such laser systems of moderate peak intensity and not-too-short pulse duration are nevertheless very good for the generation of these harmonic orders and are the best candidates

for most of the foreseen applications of this new source of coherent radiation.

REFERENCES

- ALTUCCI, C., STARCZEWSKI, T., MEVEL, E., WAHLSTRÖM, C.-G., CARRÉ, B. & L'HUILLIER, A. (1996). Influence of atomic density in high-order harmonic generation. *J. Opt. Soc. Am. B* **13**, 148–156.
- BALCOU, P. & L'HUILLIER, A. (1993). Phase-matching effects in strong-field harmonic generation. *Phys. Rev. A* **47**, 1447–1459.
- BELLINI, M., CAVALIERI, S., CORSI, C. & MATERAZZI, M. (2001a). Phase-locked, time-delayed harmonic pulses for high spectral resolution in the extreme ultraviolet. *Opt. Lett.* **26**, 1010–1012.
- BELLINI, M., CORSI, C. & GAMBINO, M.C. (2001b). Neutral depletion and beam defocusing in harmonic generation from strongly ionized media. *Phys. Rev. A* **64**, 023411, 1–10.
- BOUHAL, A., SALIÈRES, P., BREGER, P., AGOSTINI, P., HAMONIAUX, G., MYSYROWICZ, A., ANTONETTI, A., CONSTANTINESCU, R. & MULLER, H.G. (1998). Temporal dependence of high-order harmonics in the presence of strong ionization. *Phys. Rev. A* **58**, 389–399.
- LEWENSTEIN, M., SALIÈRES, P. & L'HUILLIER, A. (1995). Phase of the atomic polarization in high-order harmonic generation. *Phys. Rev. A* **52**, 4747–4754.
- L'HUILLIER, A. & BALCOU, P. (1993). High-order harmonic generation in rare gases with a 1-ps 1053-nm laser. *Phys. Rev. Lett.* **70**, 774–777.
- MIYAZAKI, K. & TAKADA, H. (1995). High-order harmonic generation in the tunneling regime. *Phys. Rev. A* **52**, 3007–3021.
- MONOT, P., AUGUSTE, T., LOMPRÉ, L.A., MAINFARY, G. & MANUS, C. (1992). Focusing limits of a terawatt laser in an underdense plasma. *J. Opt. Soc. Am. B* **9**, 1579–1584.
- RAE, S.C. (1993). Ionization-induced defocusing of intense laser pulses in high-pressure gases. *Opt. Commun.* **97**, 25–28.
- RAE, S.C., BURNETT, K. & COOPER, J. (1994). Generation and propagation of high-order harmonics in a rapidly ionizing medium. *Phys. Rev. A* **50**, 3438–3446.
- RANKIN, R., CAPJACK, C.E., BURNETT, N.H. & CORKUM, P.B. (1991). Refraction effects associated with multiphoton ionization and ultrashort-pulse laser propagation in plasma waveguides. *Opt. Lett.* **16**, 835–837.
- SAKAI, H. & MIYAZAKI, K. (1994). Effect of multiphoton ionization on high-order harmonic generation and propagation in rare gases with subpicosecond laser pulses. *Phys. Rev. A* **50**, 4204–4211.
- SALIÈRES, P., L'HUILLIER, A., ANTOINE, P. & LEWENSTEIN, M. (1999). Study of the spatial and temporal coherence of high-order harmonics. *Adv. At. Mol. Opt. Phys.* **41**, 83–93.